J|A|C|S ARTICLES

Published on Web 08/11/2009

Formation of Silicon-Based Molecular Electronic Structures Using Flip-Chip Lamination

Mariona Coll,*,†,⊥ Lauren H. Miller,† Lee J. Richter,‡ Daniel R. Hines,§ Oana D. Jurchescu,† Nadine Gergel-Hackett,† Curt A. Richter,† and Christina A. Hacker*,†

Semiconductor Electronics Division, Electronics Electrical Engineering Laboratory and Surface and Microanalysis Science Division, Chemical Science and Technology Laboratory, National Institute of Standards and Technology, Gaithersburg, Maryland 20899, and Physics Department and Laboratory for Physical Sciences, University of Maryland, College Park, Maryland 20740

Received March 3, 2009; E-mail: christina.hacker@nist.gov; mcollbau@nist.gov

Abstract: We report the fabrication of molecular electronic test structures consisting of Au-molecule-Si junctions by first forming ω-functionalized self-assembled monolayers on ultrasmooth Au on a flexible substrate and subsequently bonding to Si(111) with flip-chip lamination by using nanotransfer printing (nTP). Infrared spectroscopy (IRS), spectroscopic ellipsometry (SE), water contact angle (CA), and X-ray photoelectron spectroscopy (XPS) verified the monolayers self-assembled on ultrasmooth Au were dense, relatively defect-free, and the −COOH was exposed to the surface. The acid terminated monolayers were then reacted with a H-terminated Si(111) surface using moderate applied pressures to facilitate the interfacial reaction. After molecular junction formation, the monolayers were characterized with p-polarized backside reflection absorption infrared spectroscopy (pb-RAIRS) and electrical current−voltage measurements. The monolayer quality remains largely unchanged after lamination to the Si(111) surface, with the exception of changes in the COOH and Si−O vibrations indicating chemical bonding. Both vibrational and electrical data indicate that electrical contact to the monolayer is formed while preserving the integrity of the molecules without metal filaments. This approach provides a facile means to fabricate high-quality molecular junctions consisting of dense monolayers chemically bonded to metal and silicon electrodes.

1. Introduction

The use of organic molecules to impart electrical surface properties has been a subject of intense research not only from a fundamental perspective, but for many technological applications. In particular, organic molecules have been proposed as active components for molecular electronics,[1−3] as surface functioning agents,[4,5] and as fabrication paradigms[6−8] (i.e., utilizing molecular recognition to make complex structures).[9−11] Combining these molecular attributes with silicon is particularly of interest as there is a vast array of expertise and a substantial fabrication infrastructure available that reduces development time and enables rapid integration of molecule-based devices with conventional CMOS technology. Moreover, chemical bonding to silicon is covalent in nature, giving rise to potentially robust organic layers and low resistivity interfacial contacts.[9,12] Semiconductor doping can tailor the electronic properties of the molecular device by tuning the electronic coupling between the substrate and molecule.[13,14] Organic monolayers on semiconductors have been demonstrated to tune the substrate electrical properties for chemical and biological sensors[15,16] and to lower the operating voltage in organic semiconductor electronic devices.[17]

† Semiconductor Electronics Division, Electronics Electrical Engineering Laboratory, National Institute of Standards and Technology.
‡ Surface and Microanalysis Science Division, Chemical Science and Technology Laboratory, National Institute of Standards and Technology.
⊥ Physics Department, University of Maryland.
§ Laboratory for Physical Sciences, University of Maryland.

(1) Stewart, M. P.; Maya, F.; Kosynkin, D. V.; Dirk, S. M.; Stapleton, J. J.; McGuiness, C. L.; Allara, D. L.; Tour, J. M. *J. Am. Chem. Soc.* **2004**, *126*, 370–378.
(2) Vuillaume, D.; Boulas, C.; Collet, C.; Allan, G.; Deleru, C. *Phys. Rev. B* **1998**, *58*, 16491–16498.
(3) Lee, H. N.; Cho, J. H.; Kim, H. J. *Jpn. J. Appl. Phys.* **2003**, *42*, 6678–6682.
(4) Klauk, H.; Zschieschang, U.; Pflaum, J.; Halik, M. *Nature* **2007**, *445*, 745–748.
(5) Eves, B. J.; Fan, C.; Lopinski, G. P. *Small* **2006**, *2* (11), 1379–1384.
(6) Cui, Y.; Wei, Q. Q.; Park, H. K.; Lieber, C. M. *Science* **2001**, *293*, 1289–1292.
(7) Lopinski, G. P.; Moffatt, D. J.; Wayner, D. D. M.; Wolkow, R. A. *Nature* **1998**, *392*, 909–911.
(8) Ulman, A. *Chem. Rev.* **1996**, *96*, 1533–1554.
(9) Buriak, J. M. *Chem. Rev.* **2002**, *102* (5), 1271–1308.
(10) Wolkow, R. A. *Annu. Rev. Phys. Chem.* **1999**, *50*, 413–441.
(11) Hamers, R. J. *Annu. Rev. Anal. Chem.* **2008**, 707–736.
(12) Aswal, D. K.; Lenfant, S.; Guerin, D.; Yakhmi, J. V.; Vuillaume, D. *Anal. Chim. Acta* **2006**, *568* (1−2), 84–108.
(13) Hunger, R.; Jaegermann, W.; Merson, A.; Shapira, Y.; Pettenkofer, C.; Rappich, J. *J. Phys. Chem. B* **2006**, *110* (31), 15432–15441.
(14) He, T.; Ding, H. J.; Peor, N.; Lu, M.; Corley, D. A.; Chen, B.; Ofir, Y.; Gao, Y. L.; Yitzchaik, S.; Tour, J. M. *J. Am. Chem. Soc.* **2008**, *130* (5), 1699–1710.
(15) Swanson, P.; Gelbart, R.; Atlas, E.; Yang, L.; Grogan, T.; Butler, W. F.; Ackley, D. E.; Sheldon, E. *Sen. Actuators B* **2000**, *64* (1−3), 22–30.
(16) Guiducci, C.; Stagni, C.; Zuccheri, G.; Bogliolo, A.; Benini, L.; Samori, B.; Ricco, B. *Biosens. Bioelectron.* **2004**, *19* (8), 781–787.
(17) Aviram, A.; Ratner, M. A. *Chem. Phys. Lett.* **1974**, *29* (2), 277–283.
(18) Zhang, Q.; Archer, L. A. *J. Phys. Chem. B* **2003**, *107* (47), 13123–13132.

However, building molecular junctions on silicon has remained challenging. The strong covalent bonds at the Si surface makes self-assembly impossible due to the limited lateral mobility of the bonded molecules.[9,18] Thus dense, defect-free monolayers of bifunctional molecules are difficult to achieve.[19,20] The silicon surface is reactive toward a variety of functional groups,[21−25] making it quite challenging to get selective attachment with bifunctional molecules.[26,27] One of the largest challenges in the fabrication of reliable molecular electronic structures is the ability to make consistent contacts to the monolayer.[28−32] Instead of the idealized metal-molecule-substrate sandwich structure, traditional metal vapor-deposition often produces multiple metal filaments which diffuse through the organic monolayer and dominate the electrical response. For monolayers on silicon, metal evaporation is even more problematic as evaporated Au has been shown to displace molecules directly attached to Si.[33,34] Dense monolayers formed on silicon oxide exhibited evidence of metal penetrating the monolayer which altered the electrical response.[29,35] Because the tunneling rate of electrons is exponentially related to the distance between electrodes, electrode roughness and low density monolayers allowing partial metal penetration can also skew electrical measurements. For example, a 2% density of defects which reduces the electrode distance by 1.25 nm can carry more than 86% of the tunneling current through the molecular layer.[36] Therefore, a viable molecular electronic fabrication scheme must include a means to form dense monolayers on ultraflat electrodes and, preferentially, have molecules chemically bonded to both electrodes.

To realize reliable electrical contacts to molecular layers, it is advantageous to consider metallization methods beyond traditional metal evaporation such as soft metallization,[37−40] lift-off float-on,[41,42] or nanotransfer printing.[43−45] Nanotransfer printing (nTP) is a soft-lithography technique which is attracting much attention as a low cost method for printing nanometer-scale geometries over large areas, without having to subject the materials to harsh postprocessing conditions of etchants or sacrificial resists.[46] Recently, the capability to contact monolayers by nTP has been demonstrated by mechanically transferring Au onto the monolayers using an elastomeric stamp, typically PDMS, as a transfer substrate.[45−48] To ensure complete metal transfer to the monolayer, it is also essential to work with molecules possessing functional groups enabling a chemical bond to the metal. However, electrode roughness generates small gaps between the metal and the organic monolayer leading to unreliable electrical results.[47,49]

This work demonstrates a novel fabrication route for high-quality molecular junctions chemically bonded to silicon and ultrasmooth gold (uSAu) by using flip-chip lamination (see Figure 1). We circumvent the issues of forming dense monolayers on silicon by first self-assembling bifunctional thiols on ultrasmooth template-stripped gold substrates. Template-stripping has been widely used to prepare large areas of atomically flat surfaces[50−52] and has also been shown to be an ideal substrate to fabricate ordered monolayers.[53] Alternatively, the use of graphitic carbon substrates[54,55] and silanized SiO_2 substrates[56] has been demonstrated as smooth electrodes for molecular electronics. Our gold surface has been fabricated on a flexible polyethylene terephthalate (PET) substrate to enable conformal contact with the silicon surface. We achieve direct chemical bonding of Au-monolayers to H-terminated Si(111) under mild conditions of pressure. By means of polarized backside reflection absorption infrared spectroscopy (pb-RAIRS), we have explored the influence of pressure on

(19) Bierbaum, K.; Kinzler, M.; Woll, Ch.; Grunze, M.; Hahner, G.; Heid, S.; Effenberger, F. *Langmuir* **1995**, *11*, 512–518.
(20) Moon, J. H.; Kim, J. H.; Kim, K.-I.; Kang, T.-H.; Kim, B.; Kim, C.-H.; Hahn, J. H.; Park, J. W. *Langmuir* **1997**, *13-*, 4305–4310.
(21) Lindford, M. R.; Chidsey, C. E. D. *J. Am. Chem. Soc.* **1993**, *115*, 12631–12632.
(22) Hacker, C. A.; Anderson, K. A.; Richter, L. J.; Richter, C. A. *Langmuir* **2005**, *21* (3), 882–889.
(23) Lee, E. J.; Bitner, T. W.; Ha, J. S.; Shane, M. J.; Sailor, M. J. *J. Am. Chem. Soc.* **1996**, *118*, 5375–5382.
(24) Boukherroub, R.; Morin, S.; Sharpe, P.; Wayner, D.D. M. *Langmuir* **2000**, *16*, 7429–7434.
(25) Effenberger, F.; Gotz, G.; Bidlingmaier, B.; Wezstein, M. *Angew. Chem., Int. Ed.* **1998**, *37* (18), 2462–2464.
(26) Asanuma, H.; Lopinski, G. P.; Yu, H.-Z. *Langmuir* **2005**, *21* (11), 5013–5018.
(27) Sieval, A. B.; Linke, R.; Geij, G.; Meijer, G.; Zuilhof, H.; Sudholter, E. J. R. *Langmuir* **2001**, *17* (24), 7554–7559.
(28) Walker, A. V.; Tighe, T. B.; Cabarcos, O. M.; Reinard, M. D.; Haynie, B. C.; Uppili, S.; Winograd, N.; Allara, D. L. *J. Am. Chem. Soc.* **2004**, *126* (12), 3954–3963.
(29) Richter, C. A.; Hacker, C. A.; Richter, L. J.; Kirillov, O. A.; Suehle, J. S.; Vogel, E. M. *Solid-State Electron.* **2006**, *50* (6), 1088–1096.
(30) Tai, Y.; Shaporenko, A.; Eck, W.; Grunze, M.; Zarnikov, M. *Appl. Phys. Lett.* **2004**, *85* (25), 6257–6259.
(31) Stewart, D. R.; Ohlberg, D. A. A.; Beck, P. A.; Chen, Y.; Williams, R. S.; Jeppesen, J. O.; Nielsen, K. A.; Stoddart, J. F. *Nano Lett.* **2004**, *4* (1), 133–136.
(32) Jung, D. R.; Czanderna, A. W. *Crit. Rev. Solid State* **1994**, *19* (1), 1–54.
(33) Hacker, C. A.; Richter, C. A.; Gergel-Hackett, N.; Richter, L. J. *J. Phys. Chem. C* **2007**, *111* (26), 9384–9392.
(34) Hunger, R.; Fritsche, R.; Jaeckel, B.; Webb, L. J.; Jaegermann, W.; Lewis, N. S. *Surf. Sci.* **2007**, *601* (14), 2896–2907.
(35) Richter, C. A.; Hacker, C. A.; Richter, L. J. *J. Phys. Chem. B* **2005**, *109* (46), 21836–21841.
(36) Weiss, E. A.; Chiechi, R. C.; Kaufman, G. K.; Kriebel, J. K.; Li, Z. F.; Duati, M.; Rampi, M. A.; Whitesides, G. M. *J. Am. Chem. Soc.* **2007**, *129* (14), 4336–4349.
(37) Scott, A.; Hacker, C. A.; Janes, D. B. *J. Phys. Chem. C* **2008**, *112* (36), 14021–14026.
(38) Metzger, R. M. *J. Mater.Chem.* **2008**, *18* (37), 4364–4396.
(39) Rampi, M. A.; Whitesides, G. M. *Chem. Phys.* **2002**, *281* (2−3), 373–391.
(40) Akkerman, H. B.; Blom, P. W. M.; de Leeuw, D. M.; de Boer, B. *Nature* **2006**, *441*, 69–72.
(41) Shimizu, K. T.; Tabbri, J. D.; Jelincic, J. J.; Melosh, N. A. *Adv. Mater.* **2006**, *18* (12), 1499–1504.
(42) Vilan, A.; Cahen, D. *Adv. Funct. Mater.* **2002**, *12* (11−12), 795–807.
(43) Hsu, J. W. P. *Mater. Today* **2005**, 42–54.
(44) Hines, D. R.; Ballarotto, V. W.; Williams, E. D.; Shao, Y.; Solin, S. A. *J. Appl. Phys.* **2007**, *101* (2), 245031–245039.
(45) Loo, Y. L.; Willett, R. L.; Baldwin, K. W.; Rogers, J. A. *J. Am. Chem. Soc.* **2002**, *124* (26), 7654–7655.
(46) Gates, B. D.; Xu, Q. B.; Stewart, M.; Ryan, D.; Willson, C. G.; Whitesides, G. M. *Chem. Rev.* **2005**, *105* (4), 1171–1196.
(47) Guerin, D.; Merckling, C.; Lenfant, S.; Wallart, X.; Pleutin, S.; Vuillaume, D. *J. Phys. Chem. C* **2007**, *111* (22), 7947–7956.
(48) Loo, Y. L.; Lang, D. V.; Rogers, J. A.; Hsu, J. W. P. *Nano Lett.* **2003**, *3* (7), 913–917.
(49) Atmaja, B.; Frommer, J.; Scott, J. C. *Langmuir* **2006**, *22* (10), 4734–4740.
(50) Hegner, M.; Wagner, P.; Semenza, G. *Surf. Sci.* **1993**, *291* (1−2), 39–46.
(51) Samori, P.; Diebel, J.; Lowe, H.; Rabe, J. P. *Langmuir* **1999**, *15* (7), 2592–2594.
(52) Blackstock, J. J.; Li, M.; Freeman, R.; Stewart, D. R. *Surf. Sci.* **2003**, *546* (2−3), 87–96.
(53) Wagner, P.; Hegner, M.; Guntherodt, H. J.; Semenza, G. *Langmuir* **1995**, *11*, 3867–3875.
(54) Anariba, F.; McCreery, R. L. *J. Phys. Chem. B* **2002**, *106* (40), 10355–10362.
(55) Bergren, A. J.; Harris, K. D.; Deng, F.; McCreery, R. L. *J. Phys.: Condens. Matter* **2008**, *20* (37), 374117–374128.
(56) Mahapatro, A. K.; Scott, A.; Manning, A.; Janes, D. B. *Appl. Phys. Lett.* **2006**, *88* (15), 1519171−3.

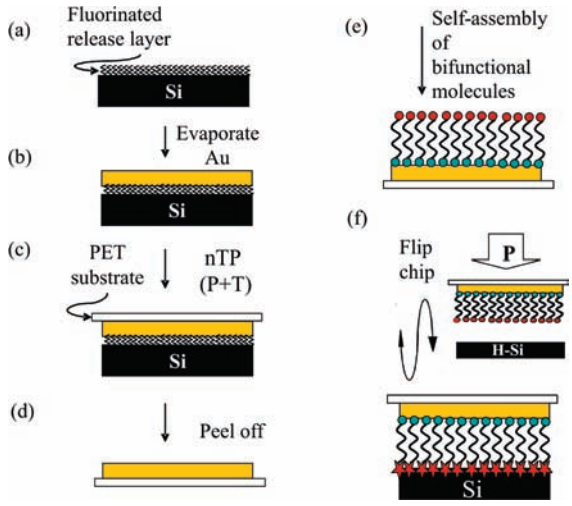

Figure 1. Schematic of flip-chip lamination process to form metal-molecule-silicon molecular junctions preserving the integrity of the molecules. Evaporated gold (b) is lifted off of a fluorinated release layer onto a PET substrate by using nTP (c) to reveal the ultrasmooth Au underside (d). Bifunctional molecules are self-assembled onto uSAu forming a dense monolayer with the functional group exposed (e). Finally, the two electrodes are laminated together with nTP causing bonding between the exposed functional group and H−Si(111) (f).

molecular conformation and interfacial reactions in the metal-molecule-silicon molecular junction. Current−voltage measurements verified electrical contact to the high-quality monolayers without formation of metal filaments or monolayer degradation. This approach is versatile and can be extended to a variety of monolayers, electrode materials, and electrode shapes. Our study provides a reliable and facile way to fabricate many molecular electronic structures in parallel. This approach can enable careful studies of the electrical properties of the organic monolayers in test structures.

2. Experimental Section

2.1. Materials and Sample Preparation. The substrates used in the present study are (i) 200 nm thick evaporated gold on silicon (precovered with 10 nm of titanium) purchased from Platypus Technologies[57] and (ii) uSAu on PET, fabricated by direct evaporation of 200 nm of gold on a Si substrate previously treated with a fluorinated release layer.[44] Transfer printing of the gold film onto the PET substrate was performed using a Nanonex 2500 imprint machine.[57] The transfer conditions were optimized to facilitate easy release of the PET layer in order to perform electrical measurements.

2.2. Monolayer Formation. All chemicals purchased are ACS grade (Octadecanethiol 99%, ODT; 11-mercaptoundecanoic acid 95%, MUA; 16-mercaptohexadecanoic acid 99%, MHA) and used as received. The uSAu/PET substrates were cut into approximately 1 cm × 1 cm squares and placed for 5 min in an ultraviolet (UV)/ozone cleaner, rinsed with water and ethanol, dried with N_2 gas, and returned to the UV/ozone cleaner for 10 min. Then substrates were placed into ethanol for 5 min and dried with N_2 gas before being immersed in 1 mmol/L alkanethiol solution overnight. The resulting samples were rinsed with 2 mol/L HCl acid at 65 °C to eliminate adsorbates and promote carboxylic acid termination in the case of MUA and MHA.

Monolayers on uSAu/PET were laminated on double side polished (DSP) hydrogen terminated- Si(111) wafers (P-doped, n-type, 10−15 Ω·cm). The H-terminated silicon substrates were prepared by immersion into a cleanroom grade buffered oxide 6:1 etch (NH_4F:HF), rinsed with 18 MΩ·cm water, and dried with nitrogen. DSP Si(111) float zone wafers (P-doped, 3000−5800 Ω·cm) were occasionally used for specific infrared spectroscopy characterization in the low frequency region, 700−1300 cm^{-1}, to avoid the contribution of interstitial oxygen contaminants. For electrical tests, DSP Si(111) (n-type, 0.001−0.005 Ω·cm) were used in order to avoid the complications associated with the Schottky barrier that can result from the energetic mismatch of the silicon and the metal, and maximize the effect of the molecular layer.

2.3. Monolayer Characterization. Gold substrates and monolayers were characterized prior to formation of the sandwich structure using contact angle, infrared spectroscopy, spectroscopic ellipsometry, scanning probe microscopy, and X-ray photoelectron spectroscopy (see Supporting Information). Following formation of the ultrasmooth metal-molecule-silicon structure, pb-RAIRS was used to characterize the molecular structure and interfacial bonding of these molecular junctions.

2.4. Atomic Force Microscopy (AFM). AFM images were acquired using a commercial AFM instrument with a deflection-type scanning head. Tapping mode images were acquired in air using Si ultrasharp tips.

2.5. Reflection Absorption Infrared Spectra (RAIRS). RAIRS were recorded using a commercial Fourier transform (FT) instrument with a liquid nitrogen cooled mercury cadmium telluride (MCT) detector (600−4000 cm^{-1}) set to 4 cm^{-1} resolution. The angle of incidence was 69° from the surface normal. SAM-uSAu/PET samples were referenced to 100 nm evaporated Au on Si and metal-SAM-Au structures were referenced to 100 nm Au evaporated on H−Si (111).

2.6. Electrical Measurements. Current−voltage (I−V) measurements were performed on patterned uSAu-monolayer Si junctions after removing the PET plastic substrate. The area of the uSAu pattern was defined by a shadow mask through which gold was evaporated on SiO_2 resulting in a device area ≈ 50 μm × 50 μm. Measurements of I−V data were acquired under nitrogen and in the dark over an applied bias range of ±1 V using a commercial probe station. Control data was acquired with the tungsten electrical probe tip in direct contact with the H−Si(111) surface.

3. Results and Discussion

The ultrasmooth gold (uSAu) surface required for flip-chip lamination is formed by first vapor depositing 200 nm of Au onto a fluorinated release monolayer on a smooth SiO_2 wafer. Nanotransfer printing (nTP) is then used to lift off the Au layer with a PET substrate exposing the uSAu surface (Figure 1a−d). AFM imaging of this uSAu surface found large uniform terraces extending several hundreds of nanometers with rms roughness of ≈0.5 nm, as shown in Figure 2a. By comparison, an AFM image of conventional evaporated Au (≈200 nm) is shown in Figure 2b with 150 nm grains and a peak-to-valley roughness of 6.5 nm (rms is ≈2.5 nm). Thus, using nTP to access the uSAu on the underside provides a starting electrode substrate which is a factor of 5 times smoother than conventional vapor-deposited Au.

High-quality monolayers can be assembled from a variety of ω-functionalized thiols by utilizing thiol-Au self-assembly. We report here the successful fabrication of Si-molecule-Au junctions via the lamination of carboxylic acid terminated self-assembled monolayers (SAMs) of 16-mercaptohexadecanoic acid (MHA) and 11-mercaptoundecanoic acid (MUA). Infrared spectroscopy (IRS), spectroscopic ellipsometry (SE), water contact angle (CA), and X-ray photoelectron spectroscopy (XPS) were used to characterize the initial SAMs, which are highly

(57) The mention or use of products in this manuscript is not meant as an endorsement by NIST nor as an indication that they are the best available.

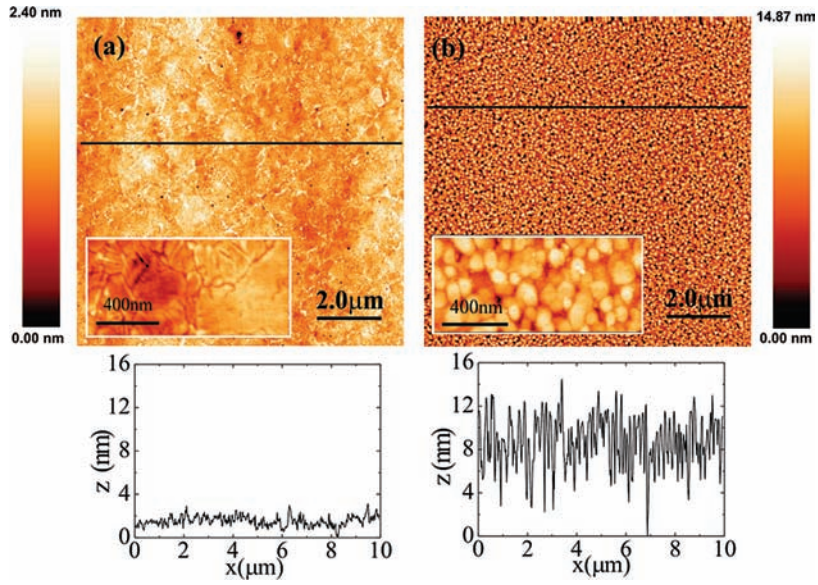

Figure 2. A 10 μm × 10 μm AFM topographic image and height profile of (a) ultrasmooth gold surface on a polyethylene terephthalate substrate (Figure 1d), and (b) evaporated gold on a silicon substrate. Black line denotes the region where height profile is performed.

ordered films with the alkane portion in an all-*trans* chain conformation and with the terminal COOH group exposed to the air surface (see Supporting Information). However, in general, the shorter chain MUA produces less ordered and less dense films, consistent with the previously reported chain length dependence of alkane thiol SAMs.[58] These dense molecular films have the terminal functional group exposed to air that can then be laminated to the ultrasmooth H-terminated Si(111) surface at room temperature under moderate pressure to create Si-molecule-Au molecular junctions (Figure 1e,f). The high-quality self-assembled monolayer and uSAu surface combined with the pliable PET substrate are promising to fabricate reproducible and reliable molecular junctions with conformal contacts by using nTP.

To evaluate adhesion between the carboxylic acid head group of the SAMs and the H−Si(111) surface, we have studied the influence of pressures up to 2 MPa at ≈30 °C. The pressures were applied to a freshly H-terminated Si(111) sample in contact with the carboxylic acid terminated SAM-uSAu substrate for a typical time of 5 min. We find a critical pressure of ≈ 0.5 MPa is necessary to achieve adhesion/reaction of the carboxylic acid terminated SAM with the H−Si(111) substrate. In fact, at $P <$ 0.5 MPa, the silicon substrate falls apart from the monolayer-uSAu/PET when the sample is removed from the imprinter. We attribute the adhesion to reaction of the acid with the silicon and is supported by the lack of adhesion at all pressures (up to 2 MPa) for ODT control films and the pb-RAIRS data. Vibrational spectra of the laminated structures were acquired after applied pressure in a pb-RAIRS setup, transmitting through the double-side polished silicon wafer and reflecting off of the Au electrode.[59] Peak positions and mode assignments are given in Table 1. In Figure 3a, the carbonyl region of the MUA monolayers assembled on uSAu before and after adhesion to H−Si(111) are compared. Before adhesion ($P <$ 0.5 MPa), the monolayer presents a single band at 1720 cm^{-1} assigned to υ(C═O) mode in H-bonded carboxylic acid groups which is commonly observed in alkanoic acid monolayers.[60,61] After adhesion, at 0.8 MPa, the spectrum contains four bands at 1725, 1627, 1558, and 1439 cm^{-1}. The first band at 1725 cm^{-1} is assigned to the carbonyl stretching mode. The peaks at 1558 and 1439 cm^{-1} are assigned to υ_{as}(OCO) and to υ_s(OCO), respectively. The presence of both modes in the IR spectra indicates the two oxygen atoms are oriented in a tilted conformation from metal surface selection rules.[62] Since only dipole moments oriented normal to the metal surface are IR active, the carboxylate group is likely interacting asymmetrically with the Si surface.[63] The frequency difference between υ_{as}(OCO) and υ_s(OCO), $\Delta\upsilon$, is sensitive to the orientation of

Table 1. IR Mode Assignments for Flip-Chip Laminated uSAu-MHA-Si and uSAu-MUA-Si

	MUA	MHA	
mode	frequency	frequency	reference
υ(C═O) H-bonded	1715 cm^{-1} 1720 cm^{-1}	1720 cm^{-1}	60, 63, 66
υ(C═O) free	1747 cm^{-1}	−	63, 66
υ(C═O), υ_{as}(OCO)	1627 cm^{-1}	−	66
υ_{as} (OCO)	1558 cm^{-1}	−	63, 66
υ(OCO)	1439 cm^{-1}	1430 cm^{-1}	63, 66
(CH_2) scissor deformation	−	1465 cm^{-1}	60, 63, 66
υ_{as}(SiO−C)	1070 cm^{-1}	1070 cm^{-1}	71, 72
υ_{as} (SiO−C)	1107 cm^{-1}	1107 cm^{-1}	71−74
υ_{as}(SiO−C)	1263 cm^{-1}	1263 cm^{-1}	71

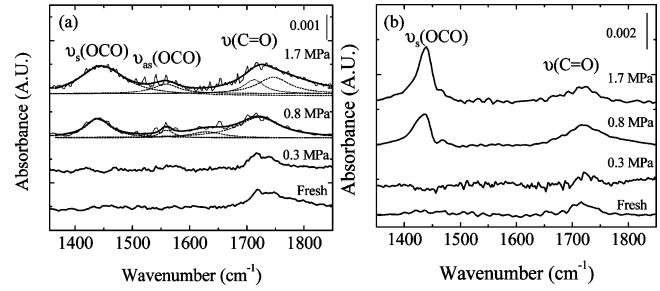

Figure 3. pb-RAIRS spectra of the carbonyl region showing the changes in the acid head group for pressures up to 2 MPa (a) uSAu-MUA (fresh) and uSAu-MUA-Si structure; (b) uSAu-MHA (fresh) and uSAu-MHA-Si. Dashed lines show the deconvolution of the MUA spectra after adhesion.

(58) Fenter, P.; Eisenberger, P.; Liang, K. S. *Phys. Rev. Lett.* **1993**, *70* (16), 2447–2450.

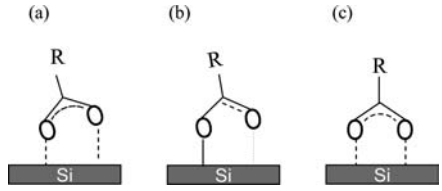

Figure 4. Schematic coordination modes proposed for the interaction of −COOH groups in the self-assembled monolayers on uSAu/PET after lamination to H−Si(111) under pressure. (a) Bidentate coordination with two oxygens interacting asymmetrically with Si, (b) Carboxylic acid group interacting to H−Si where part of the double bond character of the carbonyl group is preserved. (c) Bidentate coordination with two oxygens interacting symmetrically with Si.

O−C−O group and, therefore, is useful in identification of the bonding mode of the carboxylate group. Indeed, the observed $\Delta\upsilon$ value of ≈100 cm^{-1} matches the typical values described for a bidentate carboxylate species.[64,65] In intermediate pressure, 0.8 MPa, it is suggested that carboxylate groups are canted relative to the surface normal interacting asymmetrically with Si, as shown in Figure 4a. Further, the peak at 1627 cm^{-1} suggests the presence of a second species where the OCO of the carbonyl group preserves some double bond character which may be consistent with weak H-bonding between the C═O and the H−Si surface,[66] as depicted in Figure 4b. As the pressure increased to 1.7 MPa, the υ(C═O) mode broadens, the peak at 1627 cm^{-1} is no longer observed, and the area of the υ_s(OCO) mode increases. Therefore, it is likely that the interaction of the carboxylate group with the Si is essentially bidentate-like at 1.7 MPa, as shown in Figure 4a. The large width observed for the υ_s(OCO) suggests this peak could also contain CH_2 deformation modes which occur near 1465 cm^{-1}.[60,66] The strong υ(C═O) band can be fit to two peaks at 1715 and 1747 cm^{-1} in accordance with H-bonded and free carbonyl stretching modes.[60,63] The band at 1747 cm^{-1} might be due to either −COOH groups or an ester-like vibration Si−O-(C═O)-R.[66] These results are indicative of alteration of the H-bonding interaction between carboxylic acid groups, as expected for the formation of Si−O−C bonding. The presence of both υ(OCO) and υ(C═O) bands indicates some, but not all, carboxylic acid groups have reacted forming a chemical bond between the molecule and Si. The intensity of peaks in pb-RAIRS data is a function of the number density, orientation, and intrinsic oscillator strength. If we assume that both the carboxylate and carboxylic acid species in the MUA spectra have similar upright orientations and similar transition dipole strengths, then the relative intensities of the two modes in Figure 3a imply approximately half of the acid head groups have converted to a carboxylate at 1.7 MPa.

Figure 3b shows the IR spectra of MHA carbonyl region before and after adhesion to H−Si (111). After adhesion, the carbonyl stretch persists at 1720 cm^{-1} and a second band at lower frequency ≈1430 cm^{-1} is evident and attributable to the symmetric stretching vibration of the carboxylate functionality (OCO).[63,66] A weak feature located at 1465 cm^{-1} is also observed which is attributed to a CH_2 scissor deformation mode.[66] There is no evidence in the MHA spectra of the υ_{as}(OCO) mode, suggesting that carboxylate oxygens are oriented parallel to the surface normal, perhaps interacting with Si in a symmetric bidentate configuration as proposed in Figure 4c. With increasing pressure, the υ_s(OCO) mode becomes stronger suggesting an increase in the number of reacted COOH groups. The broadening of the υ(C═O) mode due to the appearance of the 1740 cm^{-1} contribution, also observed in the MUA spectra, indicates alteration of H-bonding among −COOH groups during the bonding with silicon, consistent with the appearance of the 1465 cm^{-1} peak. The evaluation of relative intensities of MHA carbonyl and carboxylate bands suggests about half of the carboxylic acid groups have converted to carboxylate at 1.7 MPa, similar to MUA. However, unlike MUA, MHA monolayers show a symmetric bidentate coordination of the oxygen atoms to the Si surface.

The reactivity of the terminal acid with the silicon may be determined by the original orientation of the reactive group within the SAM. Previous work has shown the orientation of terminal species, such as acid groups, is affected by the number of methylene groups (i.e., odd vs even chain length) for well-ordered monolayers.[67] It has been previously reported that MHA layers (odd-chain length) typically expose both functionalities (OH, C═O) to the air surface.[68] This configuration would give preference to a symmetric interaction of the two oxygen atoms with the H−Si(111) surface in agreement with the pb-RAIRS data. The shorter MUA monolayers are initially less ordered than MHA leading to a more heterogeneous COOH orientation. This results in no clear preference for symmetric or asymmetric reaction products in agreement with the pb-RAIRS data. The difference in reactivity of the MUA and MHA acid groups with the H−Si(111) surface is attributed to the original COOH presentation to the Si surface as determined by the quality of the molecular packing.

Figure 5 displays the IR low frequency spectra for monolayers on uSAu before lamination (a), MHA and MUA after lamination to H−Si(111) (b) and (c), respectively, and the transmission spectrum of SiO_2 (d). The Brewster's angle transmission spectrum of the native oxide surface shows the characteristic 1061 cm^{-1} Si−O−Si TO and 1226 cm^{-1} LO mode.[69,70] After Au-monolayer-Si formation, a broad feature appears at ≈ 1100 cm^{-1} which can be fit to two peaks at 1070 and 1107 cm^{-1}, shown in the inset of Figure 5. These peaks are consistent with

(59) Coll, M.; Hacker, C. A.; Miller, L. H.; Hines, D. R.; Williams, E. D.; Richter, C. A. *ECS Trans.* **2009**, *16* (25), 139–146.
(60) Allara, D. L.; Nuzzo, R. G. *Langmuir* **1985**, *1* (1), 52–66.
(61) Mitsuya, M.; Sugita, N. *Langmuir* **1997**, *13* (26), 7075–7079.
(62) Greenler, R. G. *J. Chem. Phys.* **1966**, *44* (1), 310–315.
(63) Smith, E. L.; Alves, C. A.; Anderegg, J. W.; Porter, M. D.; Siperko, L. M. *Langmuir* **1992**, *8* (11), 2707–2714.
(64) Nara, M.; Torii, H.; Tasumi, M. *J. Phys. Chem.* **1996**, *100* (51), 19812–19817.
(65) Ohe, C.; Ando, H.; Sato, N.; Urai, Y.; Yamamoto, M.; Itoh, K. *J. Phys. Chem. B* 1999, 103, 435−444.
(66) Silvernstein, R. M.; Webster, F. X. *Spectrometric Identification of Organic Compounds*, 6th ed.; John Wiley & Sons: New York, 1998; 95−99.
(67) Kim, H. I.; Houston, J. E. *J. Am. Chem. Soc.* **2000**, *122* (48), 12045–12046.
(68) Park, B.; Chandross, M.; Stevens, M. J.; Grest, G. S. *Langmuir* **2003**, *19* (22), 9239–9245.
(69) Pasternack, R. M.; Amy, S. R.; Chabal, Y. J. *Langmuir* **2008**, *24* (22), 12963–12971.
(70) Amy, S. R.; Michalak, D. J.; Chabal, Y. J.; Wielunski, L.; Hurley, P. T.; Lewis, N. S. *J. Phys, Chem. C* **2007**, *111* (35), 13053–13061.
(71) Smith, A. L. *Analysis of Silicones*, John Wiley & Sons: New York, 1974; p 271.
(72) Deshmukh, S. C.; Aydil, E. S. *J. Vac. Sci. Technol. A* **1995**, *13* (5), 2355–2367.
(73) Queeney, K. T.; Chabal, Y. J.; Weldon, M. K.; Raghavachari, K. *Phys. Stat. Sol. A* **1999**, *175* (1), 77–88.
(74) Michalak, D. J.; Rivillon, S.; Chabal, Y. J.; Esteve, A.; Lewis, N. S. *J. Phys. Chem. B* **2006**, *110* (41), 20426–20434.
(75) Salomon, A.; Bocking, T.; Gooding, J. J.; Cahen, D. *Nano Lett.* **2006**, *46* (12), 2873–2876.

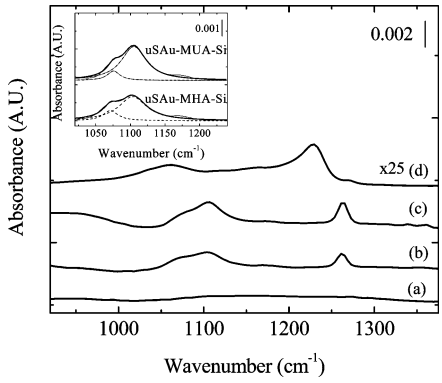

Figure 5. pb-RAIRS of the low frequency region for (a) monolayer on uSAu/PET, (b) Si-MHA-uSAu/PET, (c) Si-MUA-uSAu/PET, and (d) Transmission spectrum of native SiO_2. Inset shows a fit of the 1030−1200 cm^{-1} region for laminated MUA and MHA samples.

previous studies of ethoxy and acetoxy species adsorbed on silicon which were assigned to Si−O−C modes[71,72] supporting the linkage between the −COOH group and the H−Si surface. The Si−O−Si TO phonon mode at 1070 cm^{-1} is not expected to be observed because of surface selection rules. The absence of the strong Si−O−Si band at 1226 cm^{-1} in the molecular junction spectra suggests that minimal oxidation takes place during lamination.[73] The spectra also contain a sharp peak at 1263 cm^{-1} which has previously been attributed to a Si-CH_3 umbrella mode.[70] Lack of methyl vibrations in the pb-RAIRS data (see Supporting Information) after flip-chip lamination indicates there is minimal contamination from methyl species. Previous reports of ester compounds have also identified a Si−O−C mode in this region, which is consistent with the acid−silicon interaction.[66,71] Along with changes in Si−O and C−O vibrational spectra, the 2000−2300 cm^{-1} Si−H region (see Supporting Information) shows broadening of the 2083 cm^{-1} peak resulting from the disruption of H−Si(111) surface due to −COOH group interaction which compares well with previous studies of H−Si(111) surface reactivity.[74] We obtained molecular junctions with the organic monolayer chemically bonded to both electrodes (i.e., Au−S and Si−O−C) which facilitates the fabrication of reproducible junctions but also will allow future detailed studies of the role of molecule−electrode interface on the molecular electronic devices.[75]

Additional insight into the laminated film quality can be obtained from the CH spectral region. The inset of Figure 6 shows typical spectra obtained for MHA, MUA, and ODT with detailed analysis of the peak frequency and fwhm of the asymmetric $-CH_2-$ stretching mode (d^-) as a function of applied pressure shown in Figure 6. The control ODT spectral fwhm and peak position were nearly constant indicating the all-*trans* molecular conformation was unchanged. This is not unexpected, since pressures tens to hundreds of times greater are needed to induce irreversible chain tilting in dense monolayers.[76,77]

After compression, MHA molecules still retain a high degree of conformational order with no major structural changes. The MHA spectra show little change in d^- peak frequency with

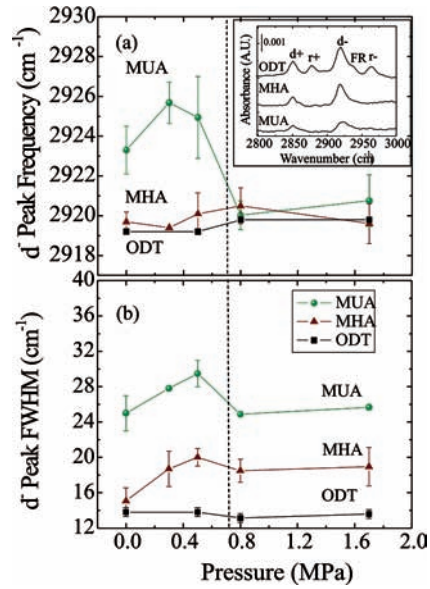

Figure 6. pb-RAIRS of ODT, MHA, and MUA monolayers on the Au-monolayer-Si structure as a function of applied pressure (a) d^- peak frequency, (b) d^- fwhm. Vibrational spectra of ODT, MHA, and MUA before flip-chip lamination are shown in the inset.

applied pressure indicating the all-*trans* configuration is maintained. The d^- fwhm broadens with increasing pressure reflecting a slight increase in disorder upon lamination, perhaps due to strain during the formation of the acid-Si bonding. The MUA monolayer, initially less dense and more conformationally disordered than MHA, orders following lamination to Si as seen by the frequency values approaching 2919 cm^{-1}. Similar irreversible annealing effects involving the removal of gauche defects were observed in the vibrational spectra of defective ODT SAMs on Au after compression ($P > 800$ MPa).[77] The reorientation of MUA monolayers at much lower pressures is likely due to a combination of the low molecular density and interaction with the Si surface providing a second anchor. Importantly, no soft CH modes near 2825 cm^{-1}, indicative of Au penetration of the films, are observed (see Supporting Information), in stark contrast with Au evaporation onto high-quality alkyl silane films.[33]

The feasibility and reliability of flip-chip lamination for electrical device fabrication has been evaluated by performing electrical measurements on patterned molecular junctions. Device areas $\approx (50 \times 50)\ \mu m^2$ were successfully flip-chip laminated with a transfer printing yield of 90%, where the printing yield is determined by visual inspection of the transferred metal after removal of the PET. However, when the device area increased $>(500 \times 500)\ \mu m^2$, the printing yield reduced to 75%. All devices that were successfully flip-chip laminated were electrically characterized, and the electrical yield was 100% for 22 devices from 6 independent fabrication runs. We examined the I−V characteristics for both MUA and MHA molecular junctions and compared them to a metal-Si control, as shown in Figure 7. MUA and MHA attenuate the current compared to the metal-Si control confirming the presence of the molecules in the junction and indicating the monolayer is acting as an ultrathin dielectric layer between the Si and Au. To compare the current density with previous molecular junctions, the resistance per molecule was estimated assuming a coverage density of 4×10^{14} molecule/cm^2. This yielded a resistance per molecule of $6.7 \times 10^6\ M\Omega \pm 0.6 \times 10^6\ M\Omega$ for

(76) Beattie, D. A.; Fraenkel, R.; Winget, S. A.; Petersen, A.; Bain, C. D. *J. Phys. Chem. B* **2006**, *110* (5), 2278–2292.
(77) Berg, O.; Klenerman, D. *J. Am. Chem. Soc.* **2003**, *125* (18), 5493–5500.
(78) Akkerman, H. B.; Bert de, B. *J. Phys.: Condens. Matter* **2008**, *20*, 013001−013021.

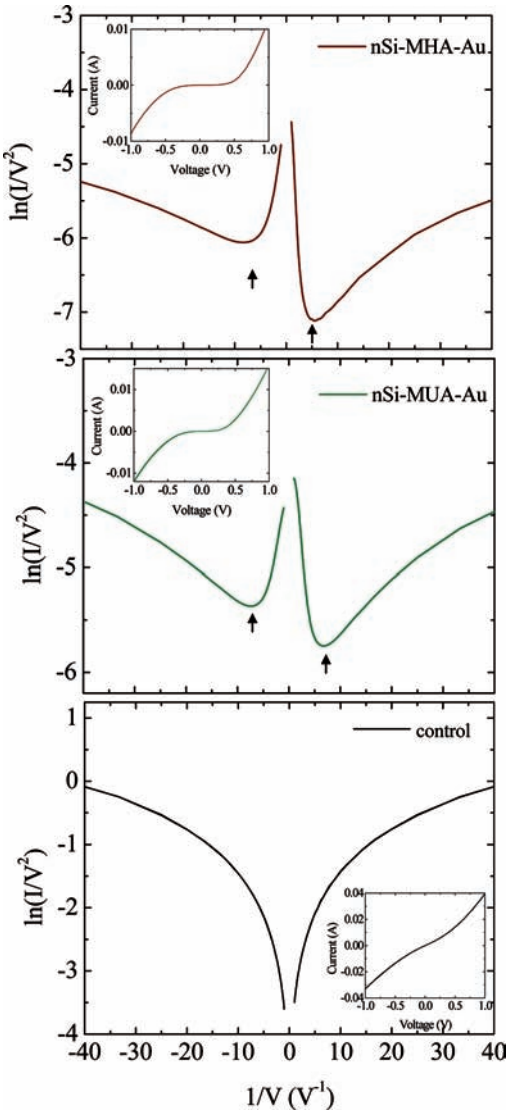

Figure 7. Transition voltage spectra of Si-MHA-uSAu molecular junctions, Si-MUA-uSAu molecular junctions and control. Arrows indicate forward and reverse bias minima in MHA and MUA molecular junctions. Insets show the linear I−V plot for the respective junctions.

MHA and 6.4×10^5 MΩ $\pm$ 0.5×10^5 MΩ for MUA. These values agree with previous data obtained from aliphatic monolayers with two chemisorbed contacts (10^4-10^6 MΩ),[78] corroborating the chemical reaction between the −COOH group and H−Si previously described in the IR data and suggests minimal metal penetration.

Transition voltage spectroscopy has been recently developed as a tool to experimentally determine the bias necessary for charge transport to transition from direct tunneling to field emission in molecular junctions.[79] The voltage at which this transition, V_{trans}, occurs is related to the height of the energy barrier between the electrode and the molecule and is therefore molecule and electrode specific.[80] The V_{trans} is identified as the minima in the Fowler-Nordheim plot (Figure 7), generated from the I−V measurements. The minima occur at $|0.17| \pm 0.02$ V for MHA and $|0.22| \pm 0.03$ V for MUA molecular junctions which is consistent with values (0.2 V) previously reported for similar silicon-alkyl junctions measured in a cross-wire configuration.[81] By contrast, the transition from tunneling to field emission occurs at much higher voltages for monolayers between metal electrodes, where V_{trans} was on the order of 1.2 V.[79] Observation of such a low transition voltage in Au-SAM-Si structures is likely due to transport facilitated by a broad density of states at the silicon interface. In addition, the asymmetric shape observed for MHA and MUA junctions agrees with Au-monolayer-Si architecture. Although detailed interpretation of the electrical data is beyond the scope of this manuscript, these electrical measurements verified electrical contact to the high-quality monolayers without formation of metal filaments or monolayer degradation.

4. Conclusions

We have developed a procedure that allows the formation of dense bifunctional monolayers bonded to both silicon and ultrasmooth gold electrodes under mild conditions. This approach offers many advantages over the conventional route of forming monolayers on silicon and evaporating a top electrode. First, monolayer formation of bifunctional molecules proceeds on the ultrasmooth gold surface via self-assembly. This facilitates the formation of dense, relatively defect-free films and allows for significantly greater flexibility in the choice of end group compared to the less selective direct attachment of bifunctional molecules to silicon. Additionally, in contrast to conventional evaporation, this approach allows us to preserve the integrity of the molecules within the junction since fabrication occurs through the application of minimal pressure, avoiding metal filament formation, monolayer degradation, and other detrimental aspects observed for traditional vapor-phase metallization of molecular layers. Our approach offers many advantages for the electrical measurement of molecules. First, our approach presents a facile means to reproducibly fabricate many junctions in parallel with high yield and fidelity allowing versatility to form devices with different sizes and shapes. Second, the ultrasmooth gold should allow better conformal contact between the two electrodes, and finally, the molecules are chemically bonded to both electrodes, minimizing the resistivity of mechanical contacts. Moreover, the flexibility of this approach can easily be extended to a variety of molecules and electrodes allowing careful study of the electrical properties of the organic monolayers.

Acknowledgment. Lauren H. Miller was supported with a National Science Foundation Summer Undergraduate Research Fellowship. Research performed in part at the nanofabrication facility within the NIST Center for Nanoscale Science and Technology. The authors thank Prof. Ellen Williams for many helpful discussions.

Supporting Information Available: Detailed experimental procedures and monolayer characterization data are available on the web. This material is available free of charge via the Internet at http://pubs.acs.org.

JA901646J

(79) Beebe, J. M.; Kim, B. S.; Gadzuk, J. W.; Frisbie, C. D.; Kushmerick, J. G. *Phys. Rev. Lett.* **2006**, *97*, 026801−026805.
(80) Beebe, J. M.; Kim, B. S.; Frisbie, C. D.; Kushmerick, J. G. *ACS Nano* **2008**, *2* (5), 827–832.
(81) Yu, L. H.; Gergel-Hackett, N.; Zangmeister, C. D.; Hacker, C. A.; Richter, C. A.; Kushmerick, J. A. *J. Phys.: Condens. Matter* **2008**, *20*, 374114–374119.